

cultured oocytes were sorted based on their sizes. Reduced representative bisulphite sequencing (RRBS) and RNA-  
2) and hypoxia (5% oxygen, 5% O<sub>2</sub>). The



## Results

### Optimisation of follicle-free oocyte culture model

To set up an oocyte *in vitro* model from immature to germinal-vesicle (GV) oocytes and to be able to manipulate oocytes sufficiently early during their development and maturation, we adopted the protocol from Honda et al. [24], which took advantage of maturing arrested primordial oocytes from dissociated ovaries of 1-week-old mice. In this method, oocytes are allowed to grow in follicle-free cultures, but initially supported by theca-like cells in the primary culture, and we considered that this method would have advantages in allowing manipulations that would be difficult to achieve in follicle cultures. Although oocytes grown by this method have been assessed as completing meiosis upon induction and to establish DNA methylation correctly for the limited number of igDMRs tested, their wider epigenetic fidelity has not been evaluated. We sought to optimise this oocyte culture system further to produce a larger quantity of GV stage oocytes for experiments. We evaluated mouse strain and age at commencement of culture (data not shown), settling on 7-day-old F<sub>1</sub>(C57BL6/BabR background) females. We included fatty acid-free bovine serum albumin (fafBSA), epidermal growth factor (EGF), and follicle stimulating hormone (FSH) in the culture medium, as these factors have been shown to improve oocyte development and maturation [25–27]. We also considered the effect of oxygen tension. Human oocytes *in vivo* are in contact with 3–5% oxygen [8], while in other mammals the oxygen concentration has been reported as being between 2 and 8% [28]. Most follicle cultures for mouse oocytes have been carried out under normoxia, with only a few studies using lower oxygen levels, such as 5% O<sub>2</sub> [9]. In this study, we compared 20% O<sub>2</sub> and 5% O<sub>2</sub> (Fig. 1a).

To evaluate the performance of the cultures, and for subsequent molecular analyses, we size-selected oocytes and categorised them into four classes by their diameters: I, < 40 μm; II, 41–49 μm; III, 51–59 μm and IV, 60–70 μm (Fig. 1a). The progression of *de novo* DNA methylation has been described in *in vivo* oocytes of similar size classes [23], which serves as a reference. In the optimised normoxia cultures, oocytes achieved a maximum diameter after 14 days, whereas in 5% O<sub>2</sub>, size IV was attained in only 9 days and after these 9 days, the oocytes started to degenerate. Under both conditions, oocytes developed into GV-like oocytes similar to *in vivo* oocytes (Fig. 1b), but the maximum sizes attained differed. An *in vivo* fully grown GV measures 70–80 μm [29], whereas in 20% O<sub>2</sub>, only 7% of the oocytes reached a size of 65 μm and in 5% O<sub>2</sub> 10% of oocytes achieved a size of 70 μm (Fig. 1c,  $p < 0.0001$ , 7 independent oocyte cultures for both conditions). The contingency graph describing the growth model showed that the number of oocytes under 20%

O<sub>2</sub> decreased slowly from class I–IV, while they grew, whereas in 5% O<sub>2</sub> the oocytes maintained their number at a plateau, when the oocytes reached the size of 50–60 μm (from class II–III) and then slowly decreased in number to reach class IV (Fig. 1d,  $n = 7$  independent oocyte cultures for both conditions).

During the final step of oogenesis, the oocyte nucleus is subject to large-scale chromatin modifications that correlate with transcriptional silencing. Oocytes that present uncondensed chromatin (NSN, non-surrounded nucleolus) are transcriptionally active, while oocytes with dense chromatin around the nucleolus are silent (SN, surrounded nucleolus); moreover, the transition to SN is required for developmental competence [30]. To define the pattern of chromatin organisation, the *in vitro*-grown oocytes were stained with DAPI and compared with *in vivo* GVs collected from 23- to 25-day-old females (3 independent oocyte cultures for both conditions, total of oocytes  $n = 68$  for 5% O<sub>2</sub> and  $n = 62$  for 20% O<sub>2</sub>). Under either culture condition, IV-class oocytes comprised both NSN and SN GVs (Fig. 1d); however, the SN oocytes grown in 20% O<sub>2</sub> had a bigger nucleolus than in 5% O<sub>2</sub>. In terms of the SN and NSN proportions, oocytes grown in 5% O<sub>2</sub> condition were closer to those of *in vivo* GV oocytes (75% SN, compared with 71% *in vivo* GV,  $n = 31$  oocytes from 23- to 25-day-old females; [30]), but only 40% of oocytes grown in 20% O<sub>2</sub> were in the SN chromatin organisation.

### Characterisation of DNA methylation in *in vitro*-grown oocytes

DNA methylation acquisition in the oocyte correlates with increasing diameter during oogenesis [23]. Therefore, the DNA methylation level of the oocytes grown under the two culture conditions was compared with the methylation of *in vivo* size-selected oocytes. We collected oocytes representing the starting populations







methylation in vivo samples but lacking methylation in





oocytes, the nuclear staining of Phospho-FOXO3A, that is seen in the untreated oocytes, is much diminished (Additional file 1: Fig. S6B,  $n=10$  oocytes for control and treated samples). Along with the staining of the cultured oocytes, GV oocytes ( $n=8$  for each condition MAO, LiCl, and control) were stained to observe the correct localisation of proteins of interest to assure that the 20% O<sub>2</sub> had no effect on the cultured oocytes (Additional file 1: Fig. S6C).

To quantify the effect of MAO and LiCl treatments on DNA methylation, we collected oocytes after 14 days of culture, grown under 20% O<sub>2</sub>, in the absence or presence of the inhibitors in triplicate pools of between 70 and 110 oocytes, and processed the oocytes for whole-genome methylation analysis by low-cell post-bisulphite adaptor-tagging (PBAT) [38, 41]. After alignment and removal of

reads from duplicates between 16,798,787 and 45,690,308 uniquely mapped reads were obtained per library. (One LiCl-treated sample was discarded because of low coverage, Additional file 2: Table S1.) For the clustering analysis, we included in this analysis, the Class IV in vivo oocyte from Gahurova et al. [23] to identify how the samples will group, as the class IV oocytes is our aimed size and present the maximum level of methylation. The

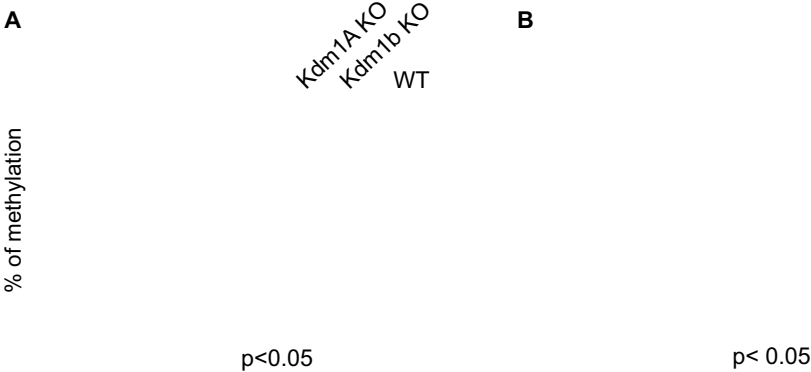
(See figure on next page.)

**Fig. 6** CGI methylation under four different conditions using oocyte in vitro model. **a** Bean plots representing total methylation in IV in vivo, IV 20% O<sub>2</sub>, MAO, LiCl, MAO + LiCl-grown oocytes and *Kdm1a*, *Kdm1b* knock-out and WT M2 oocytes, ( $\chi^2$  test,  $p < 0.05$ ). **b** Percentage of methylation at CGIs between in vivo and cultured oocytes (for IV in vivo  $n = 5707$ , IV 20% O<sub>2</sub> CON  $n = 5713$ , MAO  $n = 5713$ , LiCl  $n = 5713$ , MAO + LiCl  $n = 5713$ ,  $\chi^2$  test,  $p < 0.05$ ). **c** Heat map of the CGIs over 40% of methylation in at least one sample between the conditions, ( $n = 1138$ ;  $\chi^2$  test,  $p < 0.05$ ). **d** Distribution of CGIs over 40% of methylation in at least one sample ( $n = 1138$ ) located overlapping promoter, intragenic, and intergenic regions ( $\chi^2$  test,  $p < 0.05$ ). **e** Heatmap representing the quantitation of the methylation difference between the IV 20% O<sub>2</sub> CON compared to each cultured in vitro oocytes of the 23 igDMRs ( $\chi^2$  test,  $p < 0.05$ )

O<sub>2</sub> condition (Fig. 6A). As one of the treatments affects the activity of Kdm1 enzymes, we included the PBAT methylation datasets of *Kdm1a* and *Kdm1b* M2 knock-out oocytes from Stewart et al. [38] in the analysis. Treatments of MAO or MAO + LiCl showed a reduced CpG methylation with a pattern close to Kdm1b (data not shown). However, here we compared oocytes from different sizes (Class IV in vitro oocytes 20% O<sub>2</sub> with M2 ovulated oocytes) and could bias the results. Focussing on CGIs that normally become methylated in oocytes, we then assess the total CGIs methylation which showed a reduction in highly methylated CGIs from 1.3% ( $n = 76$ ) in 20% O<sub>2</sub> CON to nearly 0% in MAO ( $n = 32$ ), LiCl ( $n = 8$ ), and MAO + LiCl ( $n = 2$ ). The number of methylated CGI < 25% was increasing in all treated samples and was of 10% between 20% O<sub>2</sub> CON and MAO + LiCl (Fig. 6B). Then, we used the same strategy as for analysing the RBBS data, and a cut-off of > 40% methylation was used on the PBAT data set. This resulted in 1138 CGIs which clustered within 3 groups and were mostly hypomethylated in the cultured oocytes under the inhibitory drugs (Fig. 6c). They failed to properly methylate, and the proportion of CGIs localised on the promoter and intergenic regions increased compared to oocyte 20% O<sub>2</sub> CON. Most of the methylation is observed on the intragenic regions in GV oocytes [4], and the cultured oocytes presented a significant decrease in CGIs at the intragenic regions from 48% in 20% O<sub>2</sub> CON to 40% in cultured oocytes with MAO + LiCl (Fig. 6d). We also specifically evaluated effects on igDMRs, as it has previously been described that genetic ablation of *Kdm1b* in oocytes [32] impairs de novo methylation of igDMRs.

The heatmap of methylation difference of the igDMRs by comparing 20% O<sub>2</sub> CON with each drug presented a various aberrant igDMRs methylation for all the cultured oocytes (Fig. 6e). For example, *Igf2r* was highly methylated (70.1%) in IV 20% O<sub>2</sub> CON and the cultured oocytes under treatment reduced their methylation (MAO 56.5%, LiCl 38.2%, and MAO + LiCl 33.9%, respectively, Additional file 1: Fig. S7). These results suggest that the igDMRs did not gain a correct level of DNA methylation but instead obtained various levels of intermediate methylation.

Finally, we sought to assess the extent to which the treatments in vitro mimicked the ablation of *Kdm1a* and *Kdm1b* in vivo [38]. We took advantage of the published PBAT data from M2 oocytes of *Kdm1a* and *Kdm1b* knock-out mice [38]. We compared the defined hypermethylated domains (CGI over 75% methylation) of M2 oocytes knock-out mice, parameters defined in Stewart et al. [38], with our data at IV 20% O<sub>2</sub> CON oocytes > 25% methylation and the 3 other in vitro conditions (MAO, LiCl, and MAO + LiCl) over 10% of methylation. We have chosen a methylation threshold of  $\geq 25\%$  methylation for 20% O<sub>2</sub> CON ( $n = 1433$ ) as most of the CGIs had an intermediate methylation. For the other in vitro conditions MAO, LiCl, and MAO + LiCl, the methylation threshold was chosen  $\geq 10\%$  methylation to gain the maximum number of CGIs in the different culture conditions (MAO  $n = 1983$ , LiCl  $n = 2243$ , and MAO + LiCl  $n = 1817$ ). We have generated Venn diagrams to identify the overlapping CGIs between the effect of the in vitro conditions and the in vivo knock-out mice dataset. While comparing the CGIs in hypermethylated domains with in vivo CGIs of *Kdm1a* knock-out mouse hypermethylated domains, only 12 CGIs were common with all the in vitro conditions. When same comparison was carried out with the in vivo CGIs of *Kdm1b* knock-out mouse hypermethylated domains, only one CGI was common (Fig. 7a–c). In the case of the comparison with hypermethylated domains *Kdm1a* knock-out mouse, the 12 common CGIs are located mostly on intragenic regions (75%) and the remaining 25% are located on the promoter (Additional file 3: Table S2). However, in the case of non-common CGIs, we could observe an increase of CGIs located on intergenic regions for all conditions compared to *Kdm1a* and *Kdm1b* M2 knock-out oocytes (Additional file 3: Table S2). Interestingly, the CGIs in hypermethylated domains of 20% O<sub>2</sub> CON compared with hypermethylated domains of *Kdm1a* knockout oocytes ( $n = 96$ ) and the CGIs from 20% O<sub>2</sub> CON compared with hypermethylated domains of *Kdm1b* knock-out oocytes ( $n = 98$ ) were all common (Additional file 3: Table S2). These results suggest that the drugs against Kdm1 enzyme activity slowed down the gain of methylation on CGIs in grown oocytes.



## Discussion

Reproductive biology and regenerative medicine fields have made great breakthroughs to understand how to preserve fertility. Reconstitution of gametogenesis in vitro is crucial for improving and preserving fertility. To be able to reconstitute mature gametes, different alternatives have been explored to generate live offspring based on producing gametes from pluripotent stem cells [42] or from embryonic mouse germ cells

[43]. However, it is essential to prove the safety of such

Most of the follicle culture techniques are using super-ovulated oocytes (M2) [44] when they are carried on animal and human oocytes. In these culture methods, all follicles are grown with the cumulus cells around the oocytes, and the connections between the oocyte and cumulus cells are intact. In our model, few granulosa cells were attached to the immature oocytes due to the ovaries digestion step and the free theca cells resulting from the ovarian digestion formed colonies at the bottom to the Petri dish as described by Honda et al. [24]. By adding identified factors (fafBSA, EGF, and FSH) in the culture medium, known to improve oocyte development and maturation [25–27], class IV in vitro oocytes were collected. A small amount of class IV grown oocytes under 20% O<sub>2</sub> (7%) and 5% O<sub>2</sub> (10%) reached the size of GV in vivo oocytes which was the aimed size for our study. The oocytes that reached class IV under both oxygen conditions demonstrate that they complete the transition from the NSN to SN chromatin configuration to be mature oocytes [24].

Methylation in in vivo mouse oocytes was first identified to be crucial in intragenic CGI using RRBS [3] and then more recently using whole genome bisulphite sequencing via PBAT method on low amount of sample amount [21, 22, 38]. Veselovska has been demonstrating that methylation happens at the same time as transcription is occurring [4] and methylation of the last CGIs depends on the chromatin state [23]. However, the detail of the genomic distribution of methylation in in vitro mouse oocytes has not yet been clearly analysed. Here, we provide DNA methylation maps of mouse grown oocytes from immature to GV stage obtained after 9–14 days in culture under 5% O<sub>2</sub> and 20% O<sub>2</sub> condition. We observed that DNA methylation on CGIs was increased in all conditions as we could identify the methylation wave happening in the in vitro conditions. However, the hypermethylated CGIs regions were altered in the class IV in vitro oocytes in both conditions due to the oxygen concentration, 5% and 20% O<sub>2</sub>. We can hypothesise that a longer period of culture (up to 14 days) in relation to the oxygen concentration might affect the methylation status of the cytosine base and a demethylation wave might be triggered towards hydroxymethylation, resulting in hydroxymethyl cytosine and even further to the formyl cytosine. Therefore, such study needs to be carried out to portray the importance of reduced oxygen tension in the establishment of demethylation wave in in vitro-grown oocytes.

Studies exploring the influence of the duration of the culture on M2 oocytes in close contact with cumulus cells demonstrated that the blastocyst formation rate, meiosis resumption, and expression of key oocyte genes are increased [45], but their effects on imprinted genes

are currently not fully known. In our study, the two different oxygen conditions (20% vs. 5% O<sub>2</sub>) did not affect the temporal acquisition of correct imprinted DNA methylation patterns in the denuded oocytes, as the methylation of the imprinted genes was closer to the class IV in vivo oocytes as the igDMR methylation was restored in in vitro 5% and 20% O

by their interactions with the chromatin. They regulate the methylation at the hypomethylated and hypermethylated domains in oocytes [48]. We observed in our in vitro oocyte model that the localisation of Dnmt3A protein was altered in 5% O<sub>2</sub>-grown oocytes. Dnmt3A was observed in the cytoplasm in class IV in vitro oocytes, whereas it should have been localised onto the chromatin as in in vivo class IV oocytes. Such mis-localisation will lead to reduce catalytic activity of the enzyme and might explain the lower methylation level observed at the hypermethylated domain in grown oocytes.

The clinical implication of low oxygen concentration in human embryos in assisted reproductive technology has been analysed mostly at the level of embryo quality and morphology, pregnancy rate, live birth/ongoing pregnancy [49–51]. These studies show that in human low oxygen concentration might have some beneficial effect in the clinical outcomes of in vitro culture such as better pregnancy rate. So far, no studies have been conducted on analysing epigenetic marks such as DNA methylation in cultured human oocytes incubated for few hours in 5% O<sub>2</sub> or in cultured blastocysts after 4–6 days incubation at 5% O<sub>2</sub>, due to the difficulty to obtain the samples. Metadata analysis on human cohorts has hypothesised that changes in DNA methylation at specific genes during early embryo development might result in metabolic diseases in adult life such as obesity and diabetes [52]. To be able to answer such hypothesis, more studies need to be carried out to help us in understanding how DNA methylation is fully established in cultured oocytes and if any culture conditions during fertility treatments might affect the epigenome of the embryo. Therefore, whether the culture of human oocytes and embryos in low concentrations of oxygen can actually improve the clinical outcomes of ART is a question that still requires more data.

## Conclusions

In conclusion, the present study on in vitro oocyte models from immature oocytes (class IV oocytes) demonstrates that genomic DNA methylation is altered during the oocyte growth under low concentration of oxygen. Importantly, we show that CGI methylation of igDMRs is fully conserved, whereas the CGI methylation on gene bodies is disturbed due to alteration in culture conditions, here the oxygen concentration.

Therefore, from our results further study on embryos produced from immature grown oocytes under different conditions is needed to clarify whether oocyte-derived DNA methylation at igDMRs and DMRs is fully conserved and if the future embryos develop properly.

## Material and methods

### In vitro oocyte culture

The oocyte culture established by Honda et al. [24] based on stem cell factor and ES medium was optimised. In brief, the ovaries, aged of 7 days old, from C57 Black6 background breed with SV129 background mice were collected and digested with trypsin (Sigma) and collagenase I (Sigma) at 37 °C for 15 min. The trypsin-collagenase action was stopped with foetal bovine serum (Sigma) and centrifuged for 5 min at 1600 rpm. The pellet was suspended into warm medium and plated onto a gelatine coated plate. The oocyte culture was performed under two different conditions: 20% O<sub>2</sub> and 5% O<sub>2</sub> (Fig. 1a). The culture medium was changed every 24 h for the 5% O<sub>2</sub> as the colour of the medium changed rapidly to maintain the integrity of the medium composition, and every 48 h for the 20% O<sub>2</sub> condition. The grown oocytes were collected depending on their size and the culture condition and were kept in –80 °C until further process. To reach the appropriate growth size, the oocytes were grown for 9 days under 5% O<sub>2</sub> and for 14 days under 20% O<sub>2</sub>. The size of the oocytes has been grouped into classes: < 40 µm class I, 41–49 µm class II, 50–59 µm class III, and 60–70 µm class IV (Fig. 1a). For 5% O<sub>2</sub>, the size of the oocytes was collected at < 40 µm considered as class I and 60–70 µm class IV, and for 20% O<sub>2</sub>, the selected size of the oocyte was < 49 µm class II and 55–65 µm considered to be class IV as the diameter of these oocytes reached 65 µm.

Oocytes were cultured with 100 µM tranilcypromine (Sigma), a working concentration which has been shown to inhibit KDM1, and cause epigenetic changes at the promoters of specific genes [53] and with 15 mM/ml LiCl (Sigma) [35] under 20% O<sub>2</sub> condition. The control oocytes (CON) were cultured without any drugs under 20% O<sub>2</sub> condition. The oocyte cultures were stopped when the oocytes reached the size of 55–65 µm. The cultured oocytes were frozen at –80 °C until further experiments.

pairs (bps) in length were sequenced on Illumina HiSeq 2500 platform.

Post Bisulfite Amplification Treatment (PABT) libraries were generated as described previously by Peat et al. [41] for whole genome sequencing. 70–100 cultured oocytes under different treatments (Tranylcypromine, LiCl, Tranylcypromine + LiCl, and control also called 20% O<sub>2</sub> CON) with a size of 55–65 µm were used to generate the libraries in triplicate. Libraries runs were single-ended, and 100 bps in length were sequenced on Illumina HiSeq 2500 platform.

#### Preparation of RNA sequencing libraries

Total RNA from 280 cultured oocytes for each condition 20% O<sub>2</sub> and 5% O<sub>2</sub> at two different oocyte size (class IV) was extracted using trizol method (Sigma) according to the manufacturer's instructions, and the total RNA was purified using the RNA clean and Concentrator-5 kit (Zymo) followed by depletion of ribosomal RNA with Ribo-Zero magnetic kit (Illumina) to remove the ribosomal RNA. The total RNA-seq libraries were constructed according to Veselovska et al. [4]. Libraries runs, in duplicate, were sequenced as paired-ended, 100 bps in length on Illumina HiSeq 2500 platform.

#### Library mapping

Sequence alignment mapped onto the mouse genome (mm10) and methylation calls were performed using BisMark [54]. CpGs with read depth lower than 5 were discarded. We estimated bisulphite conversion rates using reads that uniquely aligned to the lambda phage genome (conversion rate over 94%). Raw reads from RNA-seq were aligned against mouse genome (mm10) and mapped using TopHat.

#### Data analysis

DNA methylation and RNA analysis were done using

## Supplementary Information

The online version contains supplementary material available at <https://doi.org/10.1186/s13148-021-01116-3>.

**Additional file 1:** Supplementary materials (Figures S1–S8).

**Additional file 2: Table S1.** Sequencing output for PBAT libraries.

**Additional file 3: Table S2.** CGIs overlapping promoter, intragenic and intergenic regions of methylated non-common CGIs after the comparison with the hypermethylated domains defined in *Kdm1a* oocytes and the CGIs methylated >25% in normoxia or 20% O<sub>2</sub> CON, and >10% in MAO, LiCl and MAO+LiCl. *PA* promoter, *In a* intragenic and *In e* intergenic.



